

# RSC Advances



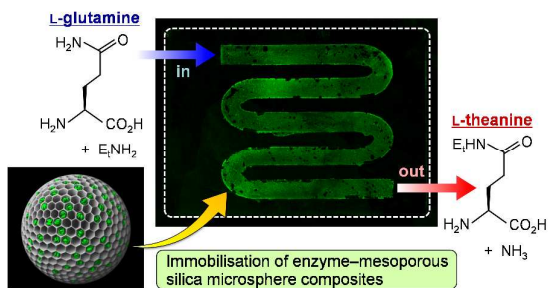
This is an *Accepted Manuscript*, which has been through the Royal Society of Chemistry peer review process and has been accepted for publication.

*Accepted Manuscripts* are published online shortly after acceptance, before technical editing, formatting and proof reading. Using this free service, authors can make their results available to the community, in citable form, before we publish the edited article. This *Accepted Manuscript* will be replaced by the edited, formatted and paginated article as soon as this is available.

You can find more information about *Accepted Manuscripts* in the [Information for Authors](#).

Please note that technical editing may introduce minor changes to the text and/or graphics, which may alter content. The journal's standard [Terms & Conditions](#) and the [Ethical guidelines](#) still apply. In no event shall the Royal Society of Chemistry be held responsible for any errors or omissions in this *Accepted Manuscript* or any consequences arising from the use of any information it contains.

## Graphical abstract



The flow-type microreactor containing composites of the enzyme (glutaminase) and mesoporous silica microspheres with a 23.6-nm pore diameter (SBA23.6) exhibited precise, efficient, and continuous synthesis of theanine.

Cite this: DOI: 10.1039/c0xx00000x

www.rsc.org/xxxxxx

PAPER

## Synthesis of amino acid using a flow-type microreactor containing enzyme–mesoporous silica microsphere composites†

Shun-ichi Matsuura,\* Manami Chiba, Emiko Tomon and Tatsuo Tsunoda

Received (in XXX, XXX) Xth XXXXXXXXX 20XX, Accepted Xth XXXXXXXXX 20XX

DOI: 10.1039/b000000x

A flow-type microreactor containing composite materials of a theanine synthetase (glutaminase) and mesoporous silica with 23.6-nm pore diameter (SBA-15 microsphere) was developed for the continuous synthesis of L-theanine, a unique amino acid. Enzyme-immobilisation ability and enzymatic activity in the SBA-15 microsphere with large mesopores were higher than those of SBA-15 with a 5.4-nm pore diameter. Moreover, the glutaminase–SBA-15 microsphere composites displayed higher selectivity in theanine production than did the free enzyme in a batch experiment. A direct visualization of composites of fluorescently labelled glutaminase and SBA-15 microsphere immobilised in the flow channel of the microreactor by a combination of differential interference contrast and fluorescence microscopy revealed that the enzymes were uniformly dispersed throughout the mesoporous silica particles, because of the successful encapsulation of the enzyme. The enzyme-encapsulated microreactor exhibited a high conversion of L-glutamine to L-theanine with local control of the reaction temperature. In addition to this advantage of the microreaction system, the microreactor enabled the on-off regulation of enzymatic activity during continuous theanine synthesis by controlling the reaction temperature or the pH of the substrate solution.

### Introduction

The development of microscale reaction technologies, such as microreactors, for use in the fields of enzyme and biological engineering has recently attracted considerable attention because of the many potential industrial applications for these technologies.<sup>1,2</sup> The advantage of using a purified, immobilised enzyme-based microreactor for biocatalytic reactions over using macro scale systems with immobilised cells is that the enzyme-immobilised microreactor facilitates the precise control of the reaction temperature to increase the reaction efficiency and reduce the reaction time.<sup>3-6</sup> The selective and stable but reversible immobilisation of an enzyme on a solid support provides a reusable, continuous reaction system and offers a promising approach for use in industrial production processes.<sup>7</sup> Despite the remarkable progress in enzyme immobilisation techniques, which rely on chemical cross-linking, physical adsorption, or specific affinity bonding, current techniques can occasionally cause severe damage to the enzymes, *e.g.*, by blocking their active centres, inducing conformational changes,<sup>8</sup> or forming aggregates. Although there are several specific enzyme immobilisation techniques using affinity bonds, such as those in the biotin–avidin system and the His-tag technique,<sup>9,10</sup> which is based on the construction of a self-assembled monolayer (SAM) of bifunctional linkers, these techniques are still very expensive and time-consuming. Therefore, a new enzyme immobilisation technique that (a) does not cause inactivation of the enzyme, (b) performs a stable, continuous reaction to yield the desired

product, and (c) is relatively cost-efficient, is desired.

In order to achieve this goal, we have developed an enzyme-encapsulated microreactor containing immobilised mesoporous silica capsules that have a hexagonally ordered pore structure,<sup>11-13</sup> which acts as an encapsulation material for delivery of proteins<sup>14</sup> and for enzymes, which is known to increase their stability and durability when exposed to heat,<sup>15,16</sup> chemicals,<sup>17</sup> pH changes,<sup>18</sup> and organic solvents.<sup>19</sup> In addition to improving the durability of the encapsulated enzyme, the effect of the pore diameter of 2D hexagonal mesoporous silica on the catalytic activities of enzymes and proteins<sup>20,21</sup> and the efficiency of energy transfer between the encapsulated proteins<sup>22-24</sup> have also been studied. Pore-size optimisation is vital for the appropriate expression of enzymatic activity in a microreactor containing composites of enzyme and mesoporous silica material. Thus, the effect of pore diameter on the adsorption capacity of silica and its reactivity toward enzymes must be clarified.

To this end, we here first investigated the ability of 2 types of SBA-15 series of mesoporous silica (SBA5.4 and SBA23.6; pore diameters of 5.4 and 23.6 nm, respectively) to encapsulate a recombinant glutaminase (theanine synthetase) and the resulting enzymatic activity in the synthesis of a unique amino acid found in tea, *viz.*,  $\gamma$ -glutamylethylamide (L-theanine), in batch experiments. Then, we conducted investigations of the on-chip encapsulation of glutaminase using the SBA-15 particles immobilised in a flow-type microreactor. We also confirmed the specific immobilisation of glutaminase on the SBA-15 particles in the microflow channel by direct visualization of the

immobilised glutaminase using optical microscopy, and subsequently evaluated the performance of the enzyme microreactor in the continuous synthesis of L-theanine.

## Experimental

### Silica source and templates

Tetraethyl orthosilicate (TEOS), as a silica source for mesoporous silicas, was obtained from Wako Pure Chemical Industries Ltd. (Osaka, Japan). Triblock copolymer, poly(ethyleneglycol)-block-poly(propylene glycol)-block-poly(ethyleneglycol) with the composition  $\text{EO}_{20}\text{PO}_{70}\text{EO}_{20}$  (Pluronic P123;  $M_w = 5800$ , Sigma-Aldrich, St. Louis, MO, USA) was used as a surfactant template. For use as a swelling agent, 1,3,5-trimethylbenzene (mesitylene) was purchased from Wako Pure Chemical Industries Ltd.

### Genes of enzyme, vector, and bacterial strain

A complete glutaminase gene derived from *Pseudomonas nitroreducens* IFO12694, which consists of 1,671 bp and encodes an enzyme of 557 amino acids,<sup>25</sup> was obtained as a synthetic gene from Life Technologies Corp. (Carlsbad, CA, USA). The vector pET302NT-His (Life Technologies Corp.) was used to clone the glutaminase gene. *E. coli* strain BL21 Star (DE3) (Life Technologies Corp.) was used as the bacterial strain for expression of enzyme.

### Preparation of mesoporous silicas

As the mesoporous silica capsules for the glutaminase, we prepared 2 types of SBA-15: SBA5.4 and SBA23.6, with pore diameters of 5.4 and 23.6 nm, respectively.

SBA5.4 was synthesized from TEOS by using Pluronic P123,<sup>26</sup> as follows. In a typical synthesis, 10 g of the Pluronic P123 was dissolved in 300 mL of water, and the resultant mixture was stirred overnight at 35 °C. Then, 21.9 g of 12 N HCl and 21.3 g of TEOS were added to the above solution. This mixture was stirred for 20 h at 35 °C. After stirring, the mixture was aged for 24 h at 35 °C.

SBA23.6 was prepared according to the method reported by Wang et al.,<sup>27</sup> with some modifications. SBA23.6 was synthesized from TEOS by using Pluronic P123 and mesitylene, as follows. To 120 mL of water was added 4 g of Pluronic P123, followed by 6.1 g of KCl; this mixture was stirred until translucent at room temperature. Then, 23.6 g of 12 N HCl and 3 g of mesitylene were added to the above solution. This mixture was stirred for 2 h at room temperature. After adding 8.5 g of TEOS to the above solution, the mixture was vigorously stirred for 10 min at room temperature, and aged for 24 h at 35 °C, and subsequently aged for another 24 h at 130 °C.

Next, the above solid products were filtered out, washed 3 times with 400 mL of distilled water at 80 °C, and dried at 45 °C. The samples were calcined in air at a heating rate of 105 °C/h and then held at 550 °C for 10 h.

### Characterization of mesoporous silicas

In order to evaluate the pore diameters, pore volumes, and specific surface areas of the calcined mesoporous silicas, nitrogen adsorption and desorption measurements were carried out at –196 °C on BELSORP-max gas adsorption apparatus (BEL Japan Inc., Osaka, Japan). The pore-size distributions were determined by analysing the adsorption branch via the Barrett-Joyner-Halenda (BJH) method.<sup>28</sup> The specific surface areas were calculated by the Brunauer–Emmett–Teller (BET) method,<sup>29</sup> using adsorption data ranging from  $P/P_0 = 0.05$  to 0.25.

To confirm the morphology of the mesoporous silica particles, scanning electron microscope (SEM) observations were carried out as follows. Scanning electron micrographs of the 2 mesoporous silicas (SBA5.4 and SBA23.6) were obtained using a Miniscope (TM-1000; Hitachi High-Technologies Corp., Tokyo, Japan) with an acceleration voltage of 15 kV.

### Preparation of recombinant glutaminase

In this study, N-terminal hexa-histidine-tagged  $\gamma$ -glutamyltranspeptidase (i.e., glutaminase) from *Pseudomonas nitroreducens* IFO12694 was overexpressed using BL21 Star *Escherichia coli* cells; subsequently, the purified enzyme was used for encapsulation in mesoporous silicas and the microflow reaction experiment.

The entire coding sequence of glutaminase was cloned into the vector pET302NT-His for expression in *E. coli*. The plasmid was introduced into *E. coli* strain BL21 Star (DE3), and the bacterial cell was grown from a single colony overnight at 37 °C in 50 mL of LB broth (Sigma-Aldrich) containing 0.1 mg/mL ampicillin. After transferring to 2,000 mL of Turbo Broth (Athena Enzyme Systems, Baltimore, MD, USA), containing 0.1 mg/mL ampicillin, and growth for 3 h at 30 °C, the cells were cultured with isopropyl  $\beta$ -D-thiogalactoside at a final concentration of 1 mM for 4 h at 30 °C. The cells were harvested by centrifugation at  $7,810 \times g$  for 5 min at 4 °C, and the pellet was washed with 400 mL of cell wash buffer (20 mM Tris (2-Amino-2-hydroxymethyl-1,3-propanediol) [ $\text{H}_2\text{NC}(\text{CH}_2\text{OH})_3$ ]-HCl buffer [pH 7.5] and 500 mM NaCl), and resuspended in 400 mL of cell lysis buffer (10 mM imidazole, 20 mM Tris-HCl buffer [pH 7.5], containing 0.05 mg/mL lysozyme, 1 mM phenylmethylsulfonyl fluoride, 500 mM NaCl, and 10 mM  $\beta$ -mercaptoethanol), and sonicated. The lysate was centrifuged at  $7,810 \times g$  for 20 min at 4 °C. The supernatant containing overexpressed enzyme was filtrated by a filter membrane with a 0.45- $\mu\text{m}$  pore size and loaded into 2-mL Ni sepharose 6 fast flow resin (GE Healthcare UK Ltd., Buckinghamshire, England) packed in a chromatography column. After loading the sample in 8 columns, the expressed enzyme was washed with wash buffer (20 mM imidazole, 20 mM Tris-HCl [pH 7.5], 500 mM NaCl, and 10 mM  $\beta$ -mercaptoethanol), and eluted with elution buffer (500 mM imidazole, 20 mM Tris-HCl [pH 7.5], 500 mM NaCl, and 10 mM  $\beta$ -mercaptoethanol). Subsequently, the sample was dialyzed with dialysis buffer (50 mM Tris-HCl [pH 7.5], 300 mM NaCl, 1 mM EDTA, 15% glycerol, 0.05% NP-40, and 5 mM  $\beta$ -mercaptoethanol), and inspissated by concentrating column.

The purified enzyme concentration was determined by the bicinchoninic acid (BCA) method, with bovine serum albumin as a standard; the purity of the enzyme was then evaluated by SDS-polyacrylamide gel electrophoresis.

### Adsorption of glutaminase to SBA mesopores

A batch adsorption experiment was performed by combining 5 mg of the mesoporous silica powder (SBA5.4 or SBA23.6) with 0.5 mL of 100 mM ethylamine hydrochloride solution (pH 5.5) containing an appropriate amount of glutaminase (0.05–2.7 mg). The glutaminase–SBA mixtures suspended in the solution were gently shaken using a rotator for 17 h at 4 °C. The glutaminase–SBA composites were then centrifuged for 5 min at  $15,300 \times g$  and the supernatant was recovered. In order to establish the amount of glutaminase adsorbed to the SBAs, the enzyme concentration of the first supernatant was determined spectrophotometrically by the BCA method, after which the amount of glutaminase adsorbed on the SBAs was determined by subtracting the concentration of the glutaminase remaining in the supernatant from that of the glutaminase before the immobilisation.

For the evaluation of enzymatic activity in the glutaminase–SBA composites in the batch experiment, the composite was rinsed twice with the above ethylamine hydrochloride solution and then resuspended in an appropriate volume of the solution so that the final concentration of the immobilised enzyme was 0.5 mg/mL.

### Preparation of a microreactor containing glutaminase–SBA composites

The proposed design of the polydimethylsiloxane (PDMS)/glass microreactor containing the glutaminase–mesoporous silica (SBA-15) composite particles is shown schematically in Figure 1. The SBA particles were immobilised over the entire surface of both sides of the slit in the microreactor, that is, the top and bottom of the flow channel, as follows. A glass substrate (width: 52 mm, length: 76 mm, thickness: 1 mm; Matsunami Glass Ind., Ltd, Osaka, Japan) was used as the base material to fabricate the flow channel of the microreactor. To immobilise SBA particles, the glass surface of the flow channel (Fig. 1a; width: 5 mm, length: 250 mm, depth: 0.2 mm), fabricated by etching the glass substrate, was coated with a thin layer of liquid PDMS prepolymer (SILPOT 184; Dow Corning Toray Co., Ltd., Tokyo, Japan) as adhesive and then sprinkled with calcined SBA powder. It was then heated for 3 h at 85 °C. The SBA particles were then immobilised onto the surface by polymerization of a PDMS prepolymer layer (thickness: 0.1 mm); as a result, the final depth of the flow channel was about 0.1 mm (inner volume: ca. 130  $\mu\text{L}$ ). Likewise, the SBA particles were immobilised on the flow channel (width: 5 mm, length: 250 mm, depth: 0.1 mm) ditched in a PDMS membrane (width: 50 mm, length: 75 mm, thickness: 1 mm) by polymerization of a PDMS prepolymer layer (thickness: 0.1 mm), resulting in a depthless flow channel. The SBA particle-immobilised surfaces of the glass channel and PDMS membrane were air-dried to remove any unattached SBA, after which the lower flow channel was sealed with the upper PDMS membrane. The flow channel was fitted with 2 microtubes for supplying solution.

Recombinant glutaminase was encapsulated in the pores of the SBA-15 immobilised in the microreactor by adding 1 mL of 100 mM ethylamine hydrochloride solution (pH 5.5) containing 0.2

mg  $\text{mL}^{-1}$  glutaminase into the flow channel at  $10 \mu\text{L min}^{-1}$  at 4 °C using a syringe pump (Model 11 plus; Harvard Apparatus, Holliston, MA, USA). The obtained glutaminase–SBA composites immobilised in the reactor were then rinsed with 1 mL of above ethylamine hydrochloride solution at  $20 \mu\text{L min}^{-1}$ .

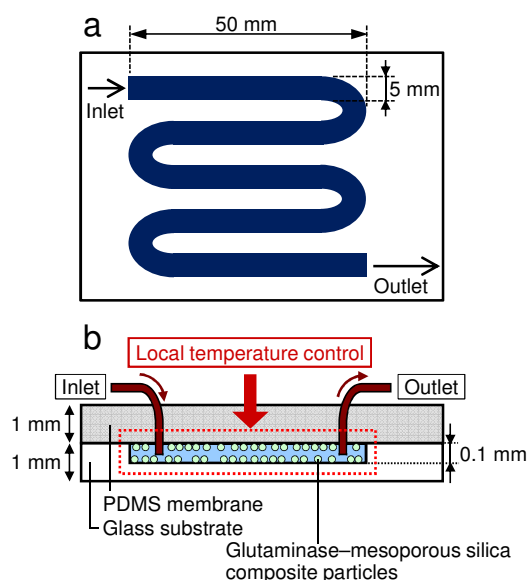


**Fig. 1** Schematic illustration of the flow-type microreactor containing immobilised glutaminase–mesoporous silica (SBA) composite particles: (a) flow channel geometry of microreactor (top view) and (b) side view of the microreactor. See also Fig. S1 (ESI<sup>†</sup>) for a detailed build process of the microreactor and a characterisation of the microflow channel.

### Visualization of glutaminase–SBA composites

To allow determination of the amount of glutaminase adsorbed onto the SBA particles, the enzyme was chemically modified with a thiol-reactive fluorescent dye (Alexa Fluor 488 C<sub>5</sub>-maleimide, C<sub>30</sub>H<sub>25</sub>N<sub>4</sub>NaO<sub>12</sub>S<sub>2</sub>;  $M_r$  720.66;  $\lambda_{\text{abs}}^{\text{max}}/\lambda_{\text{em}}^{\text{max}} = 493 \text{ nm}/516 \text{ nm}$ ; Life Technologies Corp.) at the thiol group position on the enzyme, with a degree of labelling of approximately 1 dye molecule to 1 enzyme molecule.<sup>13</sup> After preparing the fluorescently labelled enzyme, the enzyme was immobilised in the SBA-fixed microreactor by the abovementioned encapsulating and washing procedure. Then, the amount of glutaminase immobilised in each microreactor was estimated from standard curves of fluorescence intensities of Alexa 488 dye in the dye-labelled glutaminase–SBA composites (0.003–3  $\mu\text{g}$  glutaminase) using a fluorescence-image analyser (FLA-5100; FUJIFILM Corp., Tokyo, Japan).

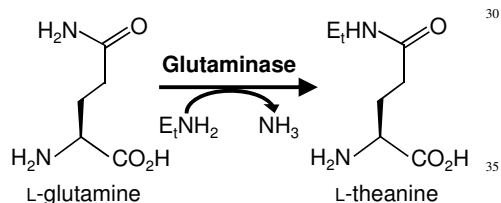
Evaluation of the encapsulation of the enzyme in SBA particles immobilised in the microreactor was also carried out by direct visualization using a fluorescence microscopy technique. The existence and relative localization of the enzyme encapsulated in the pores could be monitored by detecting the fluorescently labelled version of the enzyme.<sup>26, 30</sup> The glutaminase–SBA composites immobilised in the microreactor were observed by a combination of differential interference



contrast (DIC) and fluorescence microscopy using an inverted microscope (ECLIPSE TE2000-U; Nikon Corp., Tokyo, Japan) equipped with a 100 ×, 1.49 numerical aperture (NA) oil-immersion objective lens. The excitation and emission wavelengths were selected with the filter set GFP-BP (suitable for Alexa 488, EX480/40, DM505, and BA535/50) produced by Nikon. A fluorescence image of the labelled glutaminase was captured on an electron-multiplying charge-coupled device (EM-CCD) camera (ImagEM; C-9100-13, Hamamatsu Photonics K.K., Shizuoka, Japan) and recorded using an image processor (AQUACOSMOS analysis software; Hamamatsu Photonics K.K.). Simultaneously, the corresponding image of mesoporous silica particles, used as capsules for the enzyme, was independently obtained by DIC microscopy.

### Enzymatic reactions in batch and microreactor

Theanine synthesis by glutaminase was used as a model reaction in batch and microflow reactions. Theanine, which has been utilised as a food additive and dietary supplement, can be synthesized efficiently by a  $\gamma$ -glutamyl transfer reaction using glutaminase under basic reaction conditions (pH 10–11).<sup>25, 31</sup> Because a mixture of 2 substrates acting as a  $\gamma$ -glutamyl donor–acceptor pair is required, in this work, a combination of glutamine (donor) and ethylamine (acceptor) was used. The reaction proceeds via  $\gamma$ -glutamyl transfer from glutamine to ethylamine, with a suppression of the hydrolysis of glutamine, i.e., conversion of L-glutamine to L-theanine (Scheme 1).<sup>32, 33</sup>



**Scheme 1** Reaction scheme of L-theanine synthesis by glutaminase. The theanine is obtained by  $\gamma$ -glutamyl transfer reaction from glutamine to ethylamine with glutaminase.

The enzymatic activities of glutaminase–SBA (SBA5.4 or SBA23.6) composites in the batch experiment were measured for the synthesis reaction forming L-theanine from 2 substrates, 20 mM glutamine and 100 mM ethylamine (pH 4, 6, 8, 10, and 12). A 1.1-mL sample of the reaction mixture containing 50  $\mu$ g glutaminase in the composite form, along with the substrates, was gently shaken using a rotator for 1 h at 20 °C. The reaction was terminated by adding perchloric acid, after which glutaminase activity was evaluated by determining the amounts of L-theanine and L-glutamic acid as a by-product using a high-performance liquid chromatograph (LaChrom Elite; Hitachi High-Technologies Corp.) equipped with an octadecylsilyl-column (LaChrom C18-AQ; particle diameter: 5  $\mu$ m, Hitachi High-Technologies Corp.). The sample component was separated with the mobile phase (liquid composition;

H<sub>2</sub>O:methanol:trifluoroacetic acid = 980:20:1) at 0.5 mL min<sup>-1</sup> for 12 min at 30 °C, and the detection of L-theanine and L-glutamic acid was performed using a UV detector at 210 nm. For comparison purposes, the enzymatic activities of the free enzymes without mesoporous silica were measured. The enzymatic activity was characterised in terms of conversion ratio (CR) which is calculated using the following equation (eqn (1)):

$$\text{CR (\%)} = \frac{c(\text{theanine})}{c_0(\text{glutamine})} \times 100 \quad (1)$$

where  $c_0(\text{glutamine})$  is the initial glutamine concentration (20 mM),  $c(\text{theanine})$  is the theanine concentration after the  $\gamma$ -glutamyl transfer reaction.

In order to assess the flow system, the glutamine–ethylamine reaction solution was added to the flow channel containing the immobilised enzyme. The substrate solution (20 mM glutamine–100 mM ethylamine) was passed through the reactor at 5 or 10  $\mu$ L min<sup>-1</sup>, and the theanine synthesis by the immobilised glutaminase was carried out at various reaction temperatures (4, 10, 20, 30, 40, and 50 °C) and pH of substrate solutions (pH 4 and 10). Recovery of product solution from the outlet of the flow channel commenced after an initial 300  $\mu$ L pre-delivery delay of substrate solution using a syringe pump to reach the steady-state flow in the microreactor. In cases where the entire microreactor system, including substrate supply, the main unit of the reactor, and the product collection area, were heated (total heating), the temperature in the system was controlled using an air heat-type incubator (MIR-154; SANYO Electric Co., Ltd., Osaka, Japan). In cases where the main unit of the reactor within the microreactor system was locally heated (local heating), the temperature in the main reactor was controlled by temperature control units (Stage top incubator, INU-ONICS; Tokai Hit Co., Ltd., Shizuoka, Japan), while both the substrate supply and the product collection area were kept at 4 °C, using the air incubator mentioned above (Fig. S2, ESI<sup>†</sup>). Temperatures were made to alternate between 4 °C and 30 °C during the continuous microflow reaction by powering the temperature control units equipped with the microreactor off or on, respectively. The pH values were made to alternate between pH 4 and 10 by changing the pH of the delivery solution. After the initial 300- $\mu$ L pre-delivery, the substrate solutions were passed through the microreactor for 20 straight assays without pre-delivery solution again. After the reaction, the produced L-theanine solutions were collected from the outlet of the microreactor and the glutaminase activity was evaluated by the measuring method previously described.

## Results and discussion

### Effect of pore size of mesoporous silicas on adsorption of enzyme and the activity in batch reaction

As the mesoporous silica capsules for the enzyme, we prepared two SBA-15-type mesoporous silicas (SBA5.4 and SBA23.6). The ordered mesopores of calcined SBAs were confirmed by measuring nitrogen adsorption-desorption isotherms and the corresponding pore-size distribution curves of dried powder samples (Figure 2). The structural parameters and the SEM

images of the SBA series are shown in Table 1 and Figure 3, respectively. As shown in Table 1 and Figure 2b, the pore diameters of SBA5.4 and SBA23.6 were 5.4 nm and 23.6 nm, respectively. These data indicated that SBAs with different pore sizes were successfully prepared, although the particle morphologies of SBAs were considerably different, as is clear from the SEM images of SBA5.4 (Fig. 3a, rod-like) and SBA23.6 (Fig. 3b, sphere with 4- $\mu\text{m}$  particle diameter).

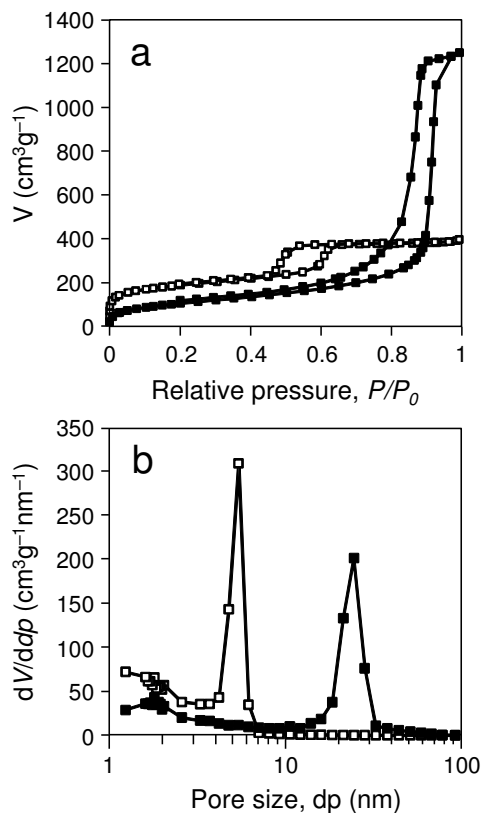


**Fig. 2** (a) Nitrogen adsorption-desorption isotherms and (b) corresponding pore size (dp) distribution curves obtained from the adsorption branch by the Barret-Joyner-Halenda (BJH) method for SBA5.4 (white squares) and SBA23.6 (black squares).

**Table 1** Structural properties of SBA-15-type mesoporous silicas.

Types of SBA-15	Pore diameter (nm)	Specific surface area (m² g⁻¹)	Total pore volume (cm³ g⁻¹)	Particle morphologies
SBA5.4	5.4	643.5	0.61	Rod
SBA23.6	23.6	470.0	2.17	Sphere

See also Fig. 2 for nitrogen adsorption-desorption isotherms and the corresponding pore size distribution curves for SBA5.4 and SBA23.6.

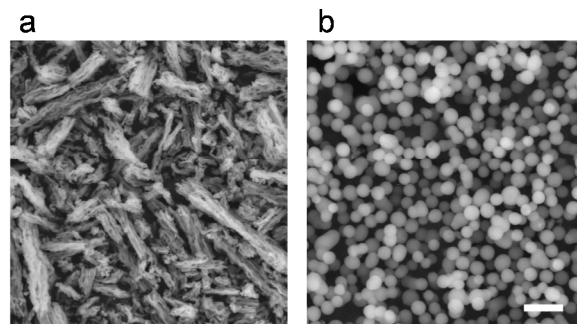


**Fig. 3** Scanning electron microscope images of SBA-15-type mesoporous silicas: (a) SBA5.4 and (b) SBA23.6. The scale bar is 10  $\mu\text{m}$ .

Before assessing theanine synthesis in the glutaminase-SBA composite contained in microreactor, batch experiments were carried out to investigate the enzyme-encapsulation efficacy and catalytic function under high pH conditions (Fig. 4). In this study, the engineered glutaminase was prepared as an enzyme solution of high purity and used for the experiments.

In encapsulation of glutaminase in the mesopores of SBAs, first, the effect of pore sizes of the 2 SBAs on the amounts of glutaminase adsorbed on the SBA pores in 100 mM ethylamine hydrochloride solution (pH 5.5) was confirmed by a batch experiment (Fig. 4a). As shown in Figure 4a, the amount of glutaminase adsorbed to SBA23.6 was notably larger than that adsorbed to SBA5.4, indicating that the amount of adsorbed enzyme was greatly dependent on the pore size of the SBAs. The proportion of glutaminase adsorbed onto the pores of the SBA23.6 was found to be up to approximately 10 wt% (by weight of SBA23.6), which was 3 times higher than that of the glutaminase adsorbed to SBA5.4. From this result, it could be surmised that it is difficult to encapsulate the enzyme easily in the pores of SBA5.4 with a 5.4-nm pore diameter, because glutaminase is approximately 5–6-nm in dimension;<sup>34</sup> that is, pores larger than the size of the enzyme is required for efficient encapsulation of enzyme. However, the maximum amount of glutaminase adsorbed on SBA23.6 (10 wt%) (Figure 4a) was lower than that adsorbed on TMPS10.6 (Taiyo Kagaku Meso Porous Silica, 10.6 nm pore diameter) (14 wt%), which was used in our previous study.<sup>13</sup> However, the TMPS10.6 was modified with a zirconia compound and then treated with 3-glycidoxypropyltrimethoxysilane to efficiently immobilise more enzyme. Although the amount of immobilised enzyme in the unmodified SBA23.6 was approximately 70% of that in modified TMPS10.6, the enzyme did not leach from the enzyme-SBA23.6 composite during the 2 wash steps despite the non-chemical surface modification of the pores. This indicates that the mesopores of the calcined SBA do not require pre-treatment (such as chemical cross-linking between the enzyme and solid support) to prevent enzyme leaching. Therefore, SBA23.6 is a relatively cost-efficient support material for reagent-free enzyme immobilisation and is superior to modified TMPS10.6.

The enzymatic activities of the obtained glutaminase-SBA composites were next measured in batch reactions (Fig. 4b) before attempting an actual microflow reaction with a

microreactor containing the composites. The batch enzymatic reactions using the glutaminase–SBA composites had to be carried out at a moderate mixing speed, because the mesoporous framework degrades under vigorous stirring because of its low mechanical strength. In the batch experiments, the enzymes that were adsorbed to mesopores of SBAs demonstrated different activities. As shown in Figure 4b, the glutaminase–SBA5.4 composite had 47.8% of the activity of the native SBA-free glutaminase in theanine production. On the other hand, the glutaminase–SBA23.6 composite had activity comparable to that of the free glutaminase (retained activity: 91.3% of that for the free enzyme), even after the adsorption. These results indicated that the difference of the pore size between SBA5.4 and SBA23.6 had a considerable effect on the activity of glutaminase under these reaction conditions. The higher remaining activity for the glutaminase–SBA23.6 composite was likely due to the larger pores of SBA23.6 and the structure of the mesoporous channels. In other words, this suggests that the strength of substrate-immobilised enzyme interactions can be enhanced by the efficient introduction of the substrate into the SBAs with larger pores. Similar results have been reported for lipase encapsulated in FSM and HOM-type mesoporous silicas.<sup>12, 16</sup> The efficiency of the glutaminase–SBA23.6 composite in synthesis of L-theanine at various reaction temperatures (a temperature range of 4–50 °C) was also of a comparable level to that of the free enzyme (Fig. S3, ESI<sup>†</sup>), indicating that the mesoporous framework of SBA23.6 did not inhibit the theanine synthesis by glutaminase regardless of the reaction temperature.

From these results, we considered that the pore size of SBA23.6 was more efficient for encapsulating glutaminase and conducting theanine synthesis. Thus, the SBA-15 microsphere (i.e., SBA23.6) was used for the subsequent enzyme encapsulation and the microflow reaction using the enzyme microreactor.

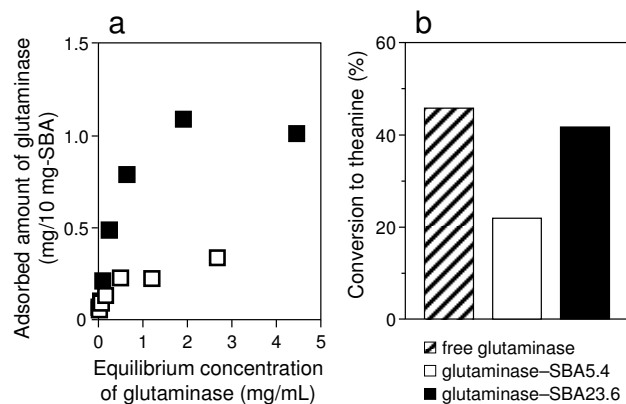


**Fig. 4** (a) Adsorption isotherms of glutaminase on SBAs. The amounts of glutaminase adsorbed to SBA5.4 (white squares) and SBA23.6 (black squares) in 100 mM ethylamine hydrochloride solution (pH 5.5) were measured spectrophotometrically with respect to the equilibrium concentrations of glutaminase. (b) Conversion of L-glutamine to L-theanine in batch reactions by free glutaminase (slash bar), glutaminase–SBA5.4 composite (white bar), and glutaminase–SBA23.6 composite (black bar). Reaction conditions: enzyme content, 50 µg; composition of

substrate, 20 mM glutamine–100 mM ethylamine (pH 10); total volume of reaction mixture, 1.1 mL; reaction time, 1 h; reaction temperature, 20 °C. See also Fig. S3 (ESI<sup>†</sup>) for effect of reaction temperature on conversion to L-theanine in batch reactions by free glutaminase and glutaminase–SBA23.6 composite.

### Evaluation of conversion and selectivity in theanine synthesis by glutaminase–SBA composites

To examine the optimal substrate solution for synthesis of L-theanine by the encapsulated enzyme, the effect of pH value of the substrate solution containing 20 mM glutamine and 100 mM ethylamine on the conversions of L-glutamine to L-theanine by free glutaminase and glutaminase–SBA23.6 composite was confirmed in batch experiments (Table 2). As shown in Table 2, theanine production was predominant at pH 10 in the cases of both free glutaminase and glutaminase–SBA23.6 composite. The optimal pH value for simultaneous hydrolysis of glutamine, i.e., conversion of L-glutamine to L-glutamic acid, was pH 8. Interestingly, conversions to L-glutamic acid as a by-product by the free glutaminase and the glutaminase–SBA23.6 composite at pH 10 were 37.7 and 2.5%, respectively. Therefore, it was found that the selectivity of L-theanine in the glutaminase–SBA23.6 composite (94.4%) was markedly higher than that of free glutaminase without SBA (54.9%) under these reaction conditions. This difference in enzymatic selectivity behaviour with and without mesoporous silica may be attributed to the difference in accessibility of water molecules to the active centre of the enzymes encapsulated in the mesopores; that is, it can be presumed that water molecules, which are required for glutamine hydrolysis, could not diffuse extensively into the pores of SBA, because of the high hydrophobicity of SBA-15-type mesoporous silica (hydrophobicity for pore surface of SBA > that of FSM).<sup>35</sup> Thus, we demonstrated the selective conversion to L-theanine by glutaminase–SBA23.6 composite as far as the theanine synthesis reaction between the glutamine, the ethylamine and the glutaminase derived from *Pseudomonas nitroreducens* is concerned.

**Table 2.** Effect of pH value of substrate solution on conversion ratio and selectivity in theanine production in batch reactions by free glutaminase and glutaminase–SBA23.6 composite.

pH of react. soln.	free glutaminase		glutaminase–SBA23.6		
	conversion theanine (%)	selectivity glutamic acid (%)	conversion theanine (%)	selectivity glutamic acid (%)	selectivity theanine (%)
4	0	11.8	0	0	-
6	0.3	70.6	0.4	0	9.0
8	0.8	78.8	1.0	0.8	16.2
10	45.8	37.7	54.9	41.8	2.5
12	0	3.0	0	0	-

Reaction conditions: enzyme content, 50 µg; composition of substrate, 20 mM glutamine–100 mM ethylamine (pH 4, 6, 8, 10, and 12); total volume of reaction mixture, 1.1 mL; reaction time, 1 h; reaction temperature, 20 °C. The conversions to L-theanine by free glutaminase and glutaminase–SBA23.6 composite at pH 10 correspond to those shown in Figure 4b.



### Direct observation of glutaminase immobilised in microreactor

In order to directly confirm the specific and stable encapsulation of glutaminase by the SBA23.6 in the flow-type microreactor, fluorescently labelled enzyme adsorbed to SBA microspheres in the reactor was observed by fluorescence microscopy containing DIC with a high-sensitivity EM-CCD camera. Figure 5 shows a picture of the enzyme microreactor fabricated in this study (Fig. 5a) and the corresponding fluorescence images of glutaminase–SBA23.6 composite particles immobilised in the microreactor (Figs. 5b and c). First, the pattern of immobilisation area for the Alexa Fluor 488 dye-labelled glutaminase in the microreactor was confirmed by scanning the entire microreactor with a fluorescence-image analyser (Fig. 5b). The area of fluorescence emission from the enzyme was distributed evenly from inlet to outlet in the microflow channel, suggesting that the distribution of the glutaminase–SBA23.6 composites in the channel was uniform. The amount of the immobilised glutaminase per unit area was estimated to be approximately 20 ng mm<sup>-2</sup> from the standard curve of fluorescence intensities of Alexa 488 dye-labelled glutaminase–SBA23.6 composites determined by the above image analyser.

We further evaluated the encapsulation and the relative localization of the glutaminase in SBA23.6 particles immobilised in the flow channel by direct visualization using optical microscopy. The fixed SBA23.6 particles with a 4-μm particle diameter in 100 mM ethylamine hydrochloride solution (pH 5.5) were successfully observed individually by DIC microscopy (Fig. 5c, upper). Next, green emission due to the Alexa 488 dye was confirmed in a same microscope field of the SBA particles when they were irradiated with an excitation light (480/40 nm; Fig. 5c, lower panel), indicating that glutaminase molecules were present in the particles. As observed from the microscopic image of the Alexa 488 dye-labelled glutaminase, the area of fluorescence emission from the enzyme was distributed evenly across the microspheres, suggesting that the distribution of glutaminase in the silica particle was uniform. This uniform distribution was attributed to the successful encapsulation of the enzyme in the SBA23.6 mesopores. As reported previously, if the labelled enzymes were adsorbed mainly on the surfaces of the mesoporous silica particles with small pore sizes, fluorescent enhancement would be obtained from the edges of the particles, because enzymes with sizes larger than the pores of the silica particles cannot penetrate beyond the entrance of the pores<sup>36</sup>. In Figure 5c (lower panel), a high signal-to-noise ratio for the image of the labelled enzymes was obtained and maintained during real-time observation, resulting from both the specific adsorption of the labelled enzyme to the silica particle rather than to the PDMS membrane in the flow channel and suppression of the leaching of the enzyme from the immobilised composite into the solution.

From the abovementioned experiments, based on the direct visualization of glutaminase–SBA23.6 composites, we presumed that the pore size of the SBA23.6 is suitable for encapsulating the enzyme and that the enzymes are indeed encapsulated in the SBA microspheres, as shown in Figure 5d.

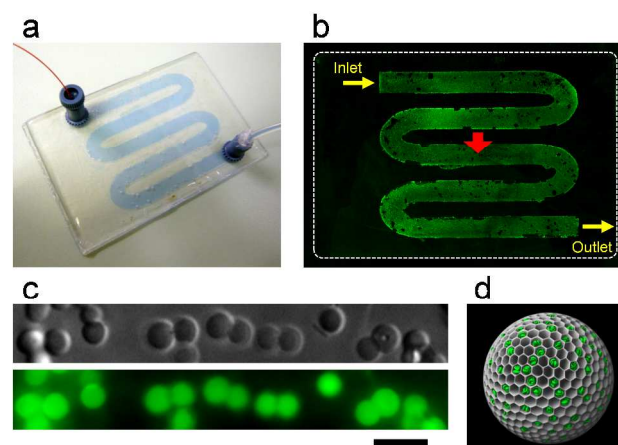


**Fig. 5** Direct visualization of glutaminase–SBA23.6 composites immobilised in microreactor: (a) picture of the microreactor, (b) the corresponding fluorescence image of Alexa 488 dye-labelled glutaminase in the microflow channel as captured by fluorescence-image analyser, (c) differential interference contrast (DIC) image of SBA23.6 particles immobilised in the flow channel (upper) and the corresponding fluorescence image of Alexa 488 dye-labelled glutaminase encapsulated in SBA23.6 (lower) observed by optical microscopy at the position indicated by a red arrow of (b), and (d) schematic illustration of enzyme–mesoporous material microsphere composite. The scale bar is 10 μm.

### Evaluation of theanine synthesis in enzyme microreactor

We next attempted to use a flow-type microreactor containing the glutaminase–SBA23.6 composites for continuous synthesis of L-theanine. In the industrial process of L-theanine production with ethylamine as a γ-glutamyl acceptor, it is necessary to carry out the synthesis reaction at a low temperature owing to the low boiling point of ethylamine (16.6 °C). Therefore, the entire microreactor system, including the substrate supply (inlet), main unit of reactor, and product collection area (outlet), were chilled to 4 °C during the theanine synthesis. Further, in order to enhance the enzymatic activity, local control of the reaction temperature (4–50 °C) in the enzyme-encapsulated microflow channel was attempted (Fig. 1b).

In the flow system in this study, first, a reaction solution containing the 2 substrates (20 mM glutamine–100 mM ethylamine, pH 10) was added into the flow channel containing the immobilised enzyme (flow rate of substrate: 10 μL min<sup>-1</sup>). We examined whether various reaction temperatures (4, 10, 20, 30, 40, and 50 °C) with total or local heating of the enzymatic reaction field in the microreactor affected the conversion to L-theanine (Fig. 6a). As is clear from the figure, interestingly, higher conversion ratios were obtained at each temperature, except for 4 °C, when the main unit of the reactor was heated with local temperature control units, compared to use of total heating. At the optimal reaction temperature (30 °C) for theanine synthesis, the conversion ratio in the case of local heating was approximately 2 times higher than that in the case of total heating. From these results, it can be speculated that the higher activity shown in local heating of the glutaminase–SBA23.6 composites in the microreactor is associated with suppression of the production of gas-phase ethylamine in the substrate supply

unit, given the low boiling point of ethylamine (16.6 °C), during the theanine synthesis reaction. From Figure 6a, it was found that the activities of the immobilised enzymes increased by local heating in the following order: 30 °C > 20 °C > 10 °C > 40 °C > 4 °C > 50 °C. On the other hand, the activity measured when the entire microreactor system, including the substrate supply, main unit of reactor, and product collection area, was heated to 40 °C, was lower than that at 4 °C, and no production of theanine was obtained at 50 °C. Furthermore, the conversion ratio at 40 °C in the case of local heating was approximately 4 times higher than that in the case of total heating, supporting the above hypothesis that the ethylamine is vaporised at a temperature range of 10–50 °C.

To investigate precise regulation of L-theanine synthesis in the continuous microflow reaction, in addition to the above advantage of local temperature control in the reaction system, we also examined the influence of changes of both reaction temperature and pH value of the substrate solution, containing 20 mM glutamine and 100 mM ethylamine, on the conversions of L-glutamine to L-theanine in a glutaminase–SBA23.6 composite-fixed microreactor (Fig. 6b). When the enzymatic activity of the immobilised glutaminase at staggered temperatures (i.e., 4 and 30 °C) during the continuous theanine synthesis at pH 10 was evaluated with local heating (flow rate of substrate: 5  $\mu\text{L min}^{-1}$ ), the glutaminase–SBA23.6 composites contained in the microreactor indicated alternately the gradual increase and decrease of the conversion to L-theanine at 30 and 4 °C, respectively. The maximum conversion ratio in this microreactor (at 30 °C and a flow rate of 5  $\mu\text{L min}^{-1}$ ) was approximately 50%, which was higher than that of the prototype enzymatic microreactor with surface-modified TMPS10.6 used in our previous study (maximum conversion ratio: ca. 10%).<sup>13</sup> When the effect of conversion to L-theanine on residence time was examined, an increase in conversion in proportion to the residence times was confirmed. A similar tendency was observed with both the glutaminase–SBA23.6 composite-fixed microreactor and the glutaminase–TMPS10.6 composite-fixed microreactor, indicating that the performance of the current enzymatic microreactor was equivalent to that of the prototype microreactor despite the non-chemical surface modification of the pores (Fig. S4, ESI<sup>†</sup>). This increased conversion in the new enzyme microreactor was due to both the improved microchannel length and the optimised pore size of the silica support for reagent-free, stable enzyme immobilisation. Moreover, we could terminate the theanine production completely by rapid cooling to the vicinity of 0 °C, resulting in temporary off-regulation of the enzymatic activity. In addition, as was the case with temperature control, alternately supplied substrate solution with a different value of pH (i.e., pH 4 and 10) led to fluctuation of the conversion. The behaviour indicated in the above results suggested that the efficiency of the enzymatic reaction could be controlled accurately by adjusting both the reaction temperature and the pH value of the substrate solution during the microflow reactions. However, the conversion ratios at the same temperature and pH range were not equivalent. This suggests that, under these experimental conditions, it was difficult to instantaneously maximize enzymatic activity by controlling the temperature and pH in the continuous microflow reaction because a specific

incubation time or substrate solution was required to reach the desired temperature and pH in areas surrounding the encapsulated enzyme. When comparing between the 2 cases, a maximum conversion ratio in the case of temperature control was clearly higher than that in the case of pH control, even when maintaining the same reaction conditions (in pH 10 at 30 °C). We considered that the lower enzymatic activity shown with the pH change is because the pH environment surrounding the active centre of the enzyme in the pores of mesoporous silica does not reach the optimal pH for theanine synthesis, owing to the particular space within the mesopores. Therefore, it can be said that the regulation of reaction temperature in the microflow reaction could affect and control enzyme activity more quickly and easily than regulation via reaction pH. The alternate on-off regulation of enzymatic activity during prolonged addition of the substrate solution in 20 assays observed in Figure 6b may be due to retention of a stable immobilised state of glutaminase; that is, it can be suggested that enzyme molecules encapsulated in the pores do not experience the reduced activity associated with the leaching of the enzyme from the flow channel during continuous reactions.

Thus, these results suggested that significant enhancement of the enzymatic activity in the enzyme–mesoporous silica composite provides the possibility of high productivity of L-theanine, by using this novel enzyme microreactor, and due to the sustained operational stability of the composites immobilised in the flow channel, which also facilitated retention of the activity of the encapsulated enzyme.

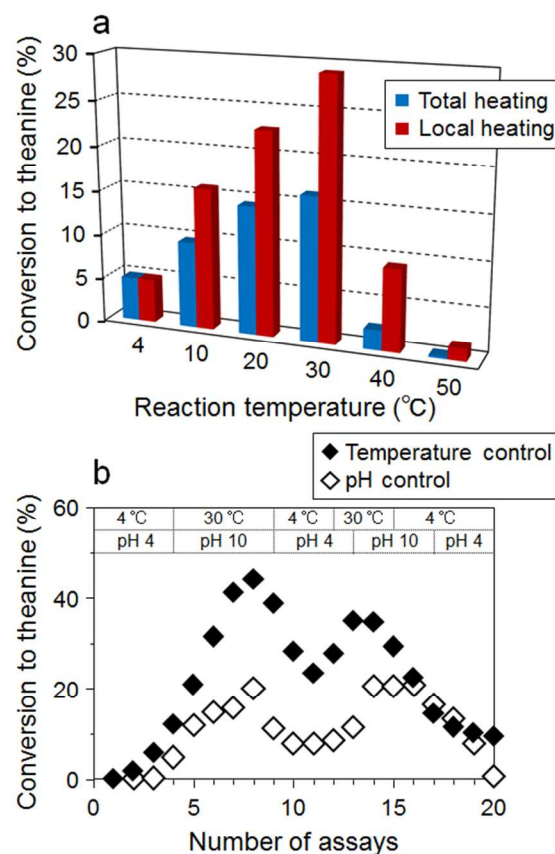


**Fig. 6** Analyses of L-theanine synthesized using a microreactor containing glutaminase–SBA23.6 composites and its temperature and pH control: (a) effect of reaction temperature with total or local heating of enzymatic reaction field in the microreactor on the conversion of L-glutamine to L-theanine. Reaction conditions: enzyme content, ca. 50 µg; composition of substrate, 20 mM glutamine–100 mM ethylamine (pH 10); flow rate of substrate solution: 10 µL min<sup>-1</sup>; reaction time, 30 min. The conversions to L-theanine were measured thrice per experimental point (*N* = 3). (b) Effect of reaction temperature and pH of substrate solution on the theanine production during the continuous reaction by local heating of enzymatic reaction field in the microreactor. Reaction conditions: composition of substrate, 20 mM glutamine–100 mM ethylamine (pH 10 constant in the case of temperature control, pH 4 or 10 in the case of pH control); reaction temperature, 4 or 30 °C in the case of temperature control, 30 °C constant in the case of pH control; flow rate of substrate solution: 5 µL min<sup>-1</sup>; reaction time, 15 min.

## Conclusions

In this study, recombinant glutaminase, derived from *Pseudomonas nitroreducens* IFO12694, was encapsulated in 2 types of mesoporous silicas (SBA5.4 and SBA23.6), and the efficient, stable immobilisation of the enzyme and its selectivity for production of L-theanine without production of L-glutamic acid as a by-product was confirmed for the glutaminase–SBA23.6 composite in batch experiments. We successfully constructed a flow-type novel microreactor containing the glutaminase–SBA23.6 composites and demonstrated the encapsulation of glutaminase in SBA23.6 particles immobilised in the microflow channel by direct visualization using an epifluorescence microscope system with DIC and demonstrated the efficiency of glutaminase–SBA23.6 composites to synthesize L-theanine. The glutaminase–SBA23.6 microreactor allowed a marked increase in conversion ratio and precise regulation of L-theanine synthesis during continuous theanine production. Control of enzyme activity was achieved by means of local heating of the reaction field in the flow channel, so avoiding effects on temperature-sensitive reactants, and by controlling the pH value of the substrate solution during solution supply. Hence, this novel microfluidic reactor system using mesoporous silica as a scaffold for enzyme-immobilisation enables efficient continuous synthesis of functional compounds, even from reactive substrates with low boiling points and low thermal stability, and effective on-off regulation of enzymatic activity by means of accurate control of the reaction temperature and the pH in the micro-reaction field.

## Acknowledgements

This research was financially supported by the Adaptable and Seamless Technology Transfer Program through Target-driven R&D (A-STEP, No. AS231Z03383E) of the Japan Science and Technology Agency (JST). The authors would like to thank Dr. Takuji Yokoyama (Taiyo Kagaku) and Dr. Takayuki Y. Nara (AIST) for providing helpful advice.

## Notes and references

Research Center for Compact Chemical System, National Institute of Advanced Industrial Science and Technology (AIST), 4-2-1 Nigatake, Miyagino-ku, Sendai 983-8551, Japan. Fax: +81-22-237-5215; Tel: +81-22-237-3039; E-mail: matsuuura-shunichi@aist.go.jp

† Electronic Supplementary Information (ESI) available: Preparation procedure and characterisation of a PDMS/glass microreactor containing an enzyme–mesoporous silica composite, photo and diagram of the experiment apparatus used for local heating, and tests for theanine production at various reaction temperatures in batch reactions by free glutaminase and glutaminase–SBA23.6 composite and at various residence times in microflow reactions using the glutaminase–mesoporous silica composites. See DOI: 10.1039/b000000x/

1. Y. Asanomi, H. Yamaguchi, M. Miyazaki and H. Maeda, *Molecules*, 2011, **16**, 6041.
2. M. Miyazaki and H. Maeda, *Trends Biotechnol.*, 2006, **24**, 463.
3. T. Honda, M. Miyazaki, H. Nakamura and H. Maeda, *Chem. Commun.*, 2005, **40**, 5062.
4. J. F. Ma, L. H. Zhang, Z. Liang, W. B. Zhang and Y. K. Zhang, *Anal. Chim. Acta*, 2009, **632**, 1.
5. M. Miyazaki, J. Kaneno, R. Kohama, M. Uehara, K. Kanno, M. Fujii, H. Shimizu and H. Maeda, *Chem. Eng. J. (Amsterdam, Neth.)*, 2004, **101**, 277.
6. M. Miyazaki, H. Nakamura and H. Maeda, *Chem. Lett.*, 2001, 442.
7. J. M. Bolivar, J. Wiesbauer and B. Nidetzky, *Trends Biotechnol.*, 2011, **29**, 333.
8. S. F. Torabi, K. Khajeh, S. Ghasempur, N. Ghaemi and S. O. R. Siadat, *J. Biotechnol.*, 2007, **131**, 111.
9. L. N. Amankwa and W. G. Kuhr, *Anal. Chem.*, 1992, **64**, 1610.
10. G. B. Sigal, C. Bamdad, A. Barberis, J. Strominger and G. M. Whitesides, *Anal. Chem.*, 1996, **68**, 490.
11. S. Matsuura, R. Ishii, T. Itoh, S. Hamakawa, T. Tsunoda, T. Hanaoka and F. Mizukami, *Mater. Lett.*, 2009, **63**, 2445.
12. S. Matsuura, R. Ishii, T. Itoh, S. Hamakawa, T. Tsunoda, T. Hanaoka and F. Mizukami, *Chem. Eng. J. (Amsterdam, Neth.)*, 2011, **167**, 744.
13. S. Matsuura, T. Yokoyama, R. Ishii, T. Itoh, E. Tomon, S. Hamakawa, T. Tsunoda, F. Mizukami, H. Nanbu and T. A. Hanaoka, *Chem. Commun.*, 2012, **48**, 7058.
14. H. S. Park, C. Kim, H. J. Lee, J. H. Choi, S. G. Lee, Y. P. Yun, I. C. Kwon, S. J. Lee, S. Y. Jeong and S. C. Lee, *Nanotechnology*, 2010, **21**, 225101.
15. I. Oda, K. Hirata, S. Watanabe, Y. Shibata, T. Kajino, Y. Fukushima, S. Iwai and S. Itoh, *J. Phys. Chem. B*, 2006, **110**, 1114.
16. S. Matsuura, S. A. El-Safty, M. Chiba, E. Tomon, T. Tsunoda and T. Hanaoka, *Mater. Lett.*, 2012, **89**, 184.
17. Y. Urabe, T. Shiomi, T. Itoh, A. Kawai, T. Tsunoda, F. Mizukami and K. Sakaguchi, *ChemBioChem*, 2007, **8**, 668.
18. P. H. Pandya, R. V. Jasra, B. L. Newalkar and P. N. Bhatt, *Microporous and Mesoporous Mater.*, 2005, **77**, 67.
19. H. Takahashi, B. Li, T. Sasaki, C. Miyazaki, T. Kajino and S. Inagaki, *Chem. Mater.*, 2000, **12**, 3301.
20. S. L. Gao, Y. J. Wang, X. Diao, G. S. Luo and Y. Y. Dai, *Bioresour. Technol.*, 2010, **101**, 3830.
21. K. Kato, M. Suzuki, M. Tanemura and T. Saito, *J. Ceram. Soc. Jpn.*, 2010, **118**, 410.
22. S. Matsuura, T. Itoh, R. Ishii, K. Sakaguchi, T. Tsunoda, T. Hanaoka and F. Mizukami, *Bioconjugate Chem.*, 2008, **19**, 10.
23. S. Matsuura, T. Itoh, R. Ishii, T. Tsunoda, K. Sakaguchi, T. Hanaoka and F. Mizukami, *Microporous and Mesoporous Mater.*, 2010, **131**, 245.
24. S. Matsuura, T. Tsunoda, T. Shiomi, K. Sakaguchi, T. Hanaoka and F. Mizukami, *Chem. Commun.*, 2010, **46**, 2941.
25. M. Imaoka, S. Yano, M. Okumura, T. Hibi and M. Wakayama, *Bioscience Biotechnology and Biochemistry*, 2010, **74**, 1936.
26. S. Matsuura, R. Ishii, T. Itoh, T. Hanaoka, S. Hamakawa, T. Tsunoda and F. Mizukami, *Microporous and Mesoporous Mater.*, 2010, **127**, 61.
27. L. N. Wang, T. Qi, Y. Zhang and J. L. Chu, *Microporous and Mesoporous Mater.*, 2006, **91**, 156.
28. E. Barrett, L. Joyner and P. Halenda, *J. Am. Chem. Soc.*, 1951, **73**, 373.

- 
29. S. Brunauer, P. Emmett and E. Teller, *J. Am. Chem. Soc.*, 1938, **60**, 309.
30. M. H. Sorensen, J. B. S. Ng, L. Bergstrom and P. C. A. Alberius, *J. Colloid Interface Sci.*, 2010, **343**, 359.
- 5 31. R. Nandakumar, K. Yoshimune, M. Wakayama and M. Moriguchi, *J. Mol. Catal. B: Enzym.*, 2003, **23**, 87.
32. T. Tachiki, T. Yamada, K. Mizuno, M. Ueda, J. Shiode and H. Fukami, *Bioscience Biotechnology and Biochemistry*, 1998, **62**, 1279.
33. F. Zhang, Q. Z. Zheng, Q. C. Jiao, J. Z. Liu and G. H. Zhao, *Amino*  
10 *Acids*, 2010, **39**, 1177.
34. T. Yokoyama, R. Ishii, T. Itoh, K. Kitahata, S.-i. Matsuura, T. Tsunoda, S. Hamakawa, T.-a. Hanaoka, H. Nanbu and F. Mizukami, *Mater. Lett.*, 2011, **65**, 67.
35. K. Hisamatsu, T. Shiomi, S. Matsuura, T. Y. Nara, T. Tsunoda, F.  
15 Mizukami and K. Sakaguchi, *J. Porous Mater.*, 2012, **19**, 95.
36. C. W. Suh, M. Y. Kim, J. B. Choo, J. K. Kim, H. K. Kim and E. K. Lee, *J. Biotechnol.*, 2004, **112**, 267.